# High-resolution measurements of the pressure broadening and shift of the rubidium $5\,^2S_{1/2}$–$6\,^2P_{3/2}$ line by argon and helium

D. Aumiler, T. Ban, and G. Pichler
*Institute of Physics, Bijenička 46, P.O. B. 304, HR-10001 Zagreb, Croatia*
(Received 8 June 2004; published 30 September 2004)

We present results of the pressure broadening and shift of the rubidium $5s\,^2S_{1/2}$–$6p\,^2P_{3/2}$ (420.2 nm) spectral line by argon and helium buffer gases at pressures below 10 torr. High-resolution absorption measurements were performed with a single-mode external cavity diode laser, having 20-GHz tuning range and a linewidth of about 1 MHz. Pressure broadening and shift parameters of Lorentzian hyperfine components have been determined. We obtained the redshift of hyperfine spectral lines for He and the blueshift for Ar.

DOI: 10.1103/PhysRevA.70.032723 PACS number(s): 34.20.−b, 32.70.Jz

## I. INTRODUCTION

The topic of broadening and shift of atomic spectral lines by collision with neutral atoms has been widely investigated in the past [1–3]. In particular, the systems of alkali metals in the presence of noble gases have been extensively studied [4], mainly due to their importance in various fields of atomic spectroscopy ranging from optical pumping experiments [5] to astrophysical applications [6]. However, most of the experimental data on the subject date from the early days of atomic spectroscopy. Advances in diode laser technology, especially in the field of external cavity diode laser (ECDL) systems, provide a new and very powerful technology that has not yet been fully applied for these kinds of investigations. The characteristics of ECDL systems, namely their single-mode tuning range of the order of tens of GHz and laser linewidth of the order of 1 MHz, show great promise for improvement over previous measurements [7].

The usual Doppler-free saturation absorption technique has proven not to be suitable for the present line-shape studies, since the crossover signals mask the hyperfine lines of interest. Therefore, here we present the results of high-resolution Doppler-limited absorption measurements of the pressure broadening and shift of the rubidium $5\,^2S_{1/2}$–$6\,^2P_{3/2}$ spectral line at 420.2 nm by argon and helium buffer gases at pressures below 10 torr. The initial motivation for this work was an accurate determination of the broadening and shift parameters, which can then be used in optical pumping experiments. Although the first rubidium resonance doublet in the presence of noble gases has been thoroughly investigated [8–10], the only available second resonance doublet pressure broadening and shift data go back to the work of Ny and Ch'en [11], which involved only high noble gas pressures of the order of tens of atmospheres.

## II. EXPERIMENTAL SETUP

A crossed heat-pipe oven (HPO) was used for the generation of rubidium vapor. It was made from two stainless-steel pipes 140 and 170 mm long, with 16-mm inner diameter. The pipe ends were closed with four quartz windows and connected to a vacuum system and He and Ar gas sources. The buffer-gas pressure was controlled with a MKS Baratron 722A manometer. A Thermocoax heater wound up around the center of the heat-pipe oven was connected to a stabilized power supply, providing stabile temperature conditions for the system. The temperature was measured using a Thermocoax thermocouple placed outside the heat pipe oven, as close to its center as possible.

A linear all-sapphire cell (ASC) [12,13], filled with pure rubidium metal, was used as a reference cell. The ASC was 120 mm long, with 10.4-mm inner diameter and 13.5-mm outer diameter. The temperature was measured by three thermocouples placed at the central point and two side points of the cell, in contact with the outer wall of the cell (for a detailed analysis of the temperature determination, see Ref. [13]).

To ensure optimum optical line thickness, the temperature of the ASC cell was 363 K, whereas the HPO temperatures were 368 K for helium and 358 K for argon buffer-gas measurements.

For the determination of the pressure broadening and shift, simple diode laser absorption measurements were performed. We used a Toptica DL 100 external cavity diode laser (ECDL) system [14], equipped with an NLHV3000E laser diode with a wavelength of approximately 420 nm and a maximum output power of 16 mW. This laser system provides a continuous single-mode tuning range of over 20 GHz, with a linewidth of the order of 1 MHz. Due to the large transition probability of the resonance line, the laser intensity had to be strongly reduced to avoid optical pumping effects. This was achieved by means of neutral filters, so the laser intensity used in the experiment was less than $1\ \mu\mathrm{W/mm^2}$.

A Fabry-Perot etalon was used to control the single-mode operation of the laser diode. Without the piezoscanning, the etalon provides reference marker fringes corresponding to the continuous laser frequency scan. Due to the relatively low free-spectral range of 2 GHz, the etalon was primarily used for determination of any possible nonlinearity in the laser frequency scan. More accurate frequency calibration of the spectra was achieved through a comparison of the reference cell spectra with the theoretical calculations, as discussed in Sec. III.

The data-acquisition system consisted of a laboratory computer connected to the analog-digital oscilloscope. The

 

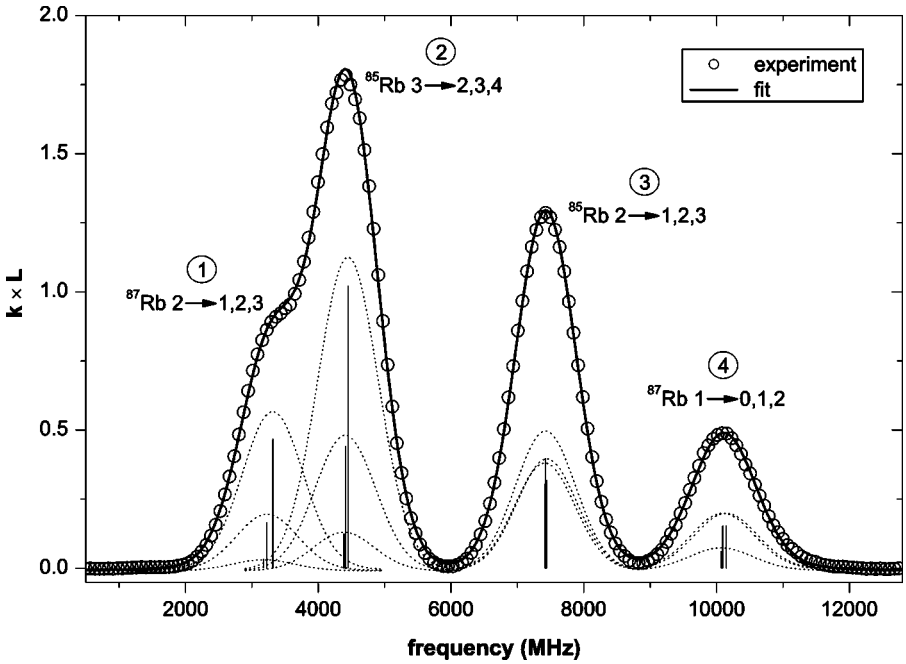


FIG. 1. Absorption profile of the Rb $5\,^2S_{1/2}$–$6\,^2P_{3/2}$ line: circles, measured reference cell profile (the actual number of data points measured is reduced for clarity); full line, fit result (hyperfine lines forming the total absorption profile are also shown as dotted lines); vertical lines, relative intensities and frequency offsets of hyperfine lines.

oscilloscope records the signal from two photodiodes, which measure laser transmission intensities in the HPO and the reference cell (ASC). In order to increase the frequency resolution given by the fixed number of 2046 data points taken in each scan, the typical scan width was about 15 GHz, which was enough for the full scan of the $5\,^2S_{1/2}$–$6\,^2P_{3/2}$ line. Simultaneous data acquisition of the transmission signal in the HPO and the reference cell, and also of the etalon marker fringes, was performed.

### III. DATA ANALYSIS

On the basis of transmission through the HPO and the reference cell, using Beer-Lambert's law, absorption spectra were calculated. The absorption profiles consist of four lines, two of them resulting from $^{85}$Rb absorption and the other two from $^{87}$Rb (Fig. 1). Two lines corresponding to each rubidium isotope are a result of the hyperfine splitting of the Rb ground $5\,^2S_{1/2}$ level, which is 3036 MHz for $^{85}$Rb and 6835 MHz for $^{87}$Rb, as shown in Fig. 2. The hyperfine lines resulting from the splitting of the upper $6\,^2P_{3/2}$ level are not resolved due to Doppler broadening, which, in our experimental conditions, is approximately 1000 MHz.

In order to calculate the pressure broadening and shift parameters from the measured absorption spectra, a numerical custom-written line-shape fitting routine was developed. A Voigt profile fitting procedure that includes all the hyperfine transitions relevant for the formation of the observed absorption profiles was used. The program performs a general nonlinear least-squares fit to the Voigt profile, based on the Humlíček algorithm [15] for rapid calculation of the Voigt function and its derivatives.

The Voigt profile is calculated for all 12 possible hyperfine transitions, given by the selection rule $\Delta F=0,\pm 1$ (Fig. 1). The contributions from the individual hyperfine lines are then added to give the total absorption spectrum. Fixed parameters are ground $5\,^2S_{1/2}$ and excited $6\,^2P_{3/2}$ state hyperfine splittings [16], together with the relative intensities of each hyperfine component [17]. Free parameters include the Lorentzian FWHM (full width at half maximum) and frequency shifts. However, not all 12 widths and shifts of hyperfine transitions could be set as free parameters, as the fitting function given by 24 free parameters altogether could not provide physically meaningful results. Therefore, three lines corresponding to a particular ground-state hyperfine level were assumed to have equal Lorentzian widths and their relative frequency offset was assumed to follow the initial excited-state hyperfine splitting. In this way, we were able to calculate independently the pressure broadening and shift of the $^{87}$Rb $F=2\rightarrow 1,2,3$, $^{85}$Rb $F=3\rightarrow 2,3,4$, $^{85}$Rb $F=2\rightarrow 1,2,3$, and $^{87}$Rb $F=1\rightarrow 0,1,2$ lines for the rubidium $5\,^2S_{1/2}$–$6\,^2P_{3/2}$ (420.2 nm) second resonance line.

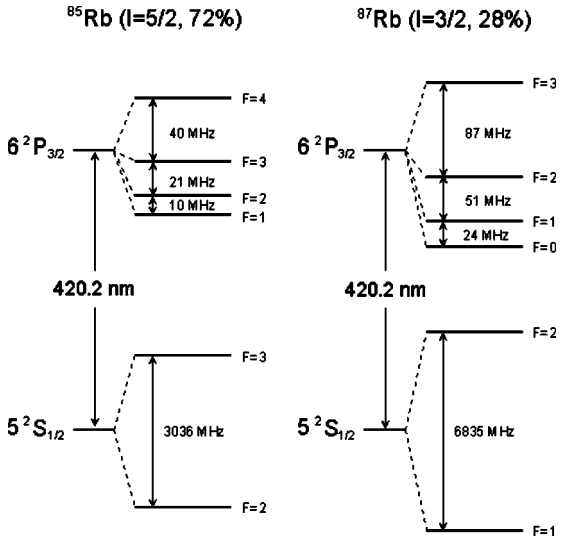


FIG. 2. Hyperfine structure of the Rb $5\,^2S_{1/2}$–$6\,^2P_{3/2}$ line.

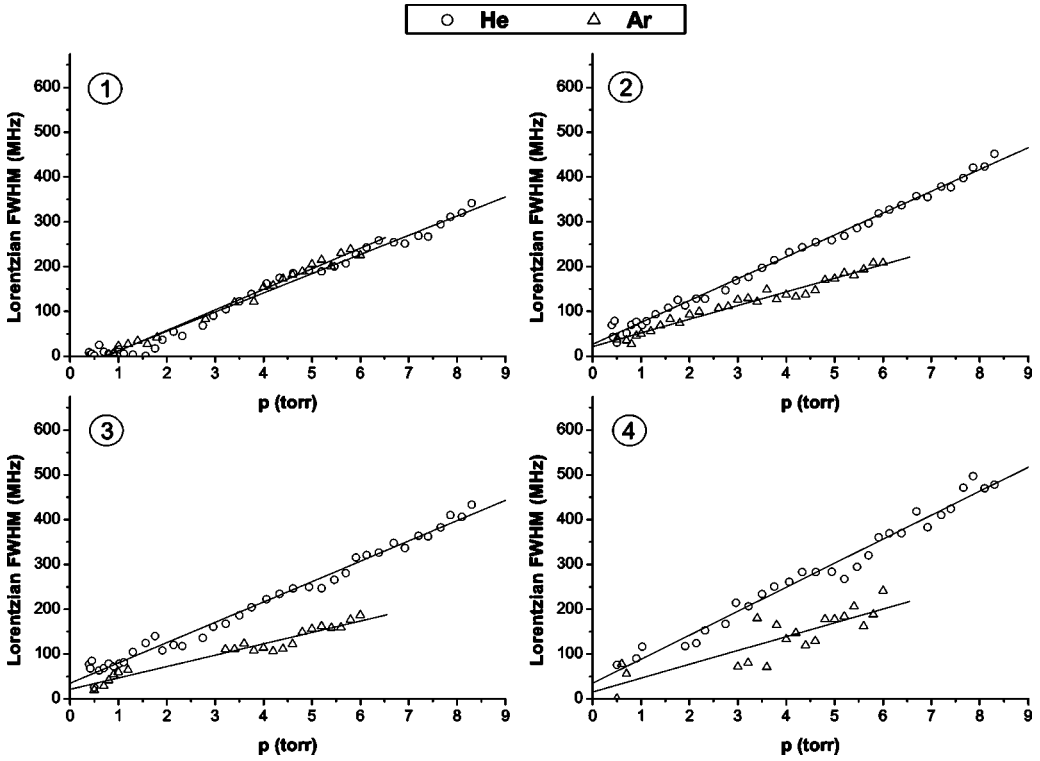


FIG. 3. The pressure broadening results of the Rb $5\,^2S_{1/2}$–$6\,^2P_{3/2}$ line in He and Ar (hyperfine line notation the same as in Fig. 1).

In all calculations, the Doppler width was included as a fixed parameter since the trade-off between the Doppler and Lorentzian widths can be significant in the fitting function. Holding the Doppler width fixed greatly improves the quality of the fitting results and is justified by the fact that the vapor temperature was held stable during the measurements. Typically, the temperature variations during consecutive scans were less than 1 K, corresponding to Doppler width variations of less than 0.2%.

The calibration of the frequency scale was made by comparison of the measured reference cell absorption spectra with the theoretical calculated spectra. The theoretical spectra were calculated using the same numerical routines as in the fitting procedure, by including all hyperfine transitions as Voigt profiles to form the resulting absorption profile. The parameters in the calculation included natural widths [18] and relative intensities of all hyperfine components, hyperfine splittings, and relevant isotope shifts [19]. Doppler width was calculated from the reference cell temperature. In this way, the absorption spectra were calculated and compared with the measured ones. The frequency axis of the reference cell measured data was then modified until exact overlap of the calculated and measured reference cell absorption spectra was obtained. By doing so, the frequency axes of the measured absorption spectra were calibrated separately for each buffer-gas pressure measurement.

## IV. RESULTS AND DISCUSSION

The results of pressure broadening and shift of the Rb $D_2$ second resonance line hyperfine components by He and Ar buffer gases are shown in Figs. 3 and 4. The values for the pressure broadening are determined from linear fits of the Lorentzian widths (FWHM), as a function of the buffer-gas pressure. The frequency differences in the line centers in the reference cell and the HPO absorption spectra give the values of frequency shift. Linear fits of the frequency shifts, as a function of the buffer-gas pressure, determine the values of pressure shift parameters. The results are shown in Table I.

The Lorentzian widths show a linear dependence on the buffer-gas pressure (Fig. 3), with the linear fit slope giving the pressure broadening parameter value (Table I). In addition to the linear fit errors, the total errors are also listed in Table I. The total error of the pressure broadening and shift parameters comprises, besides the linear fit error, the statistical error of the fitting procedure of less than 1%, and the error due to the Gaussian-Lorentzian width trade-off given by the uncertainty in temperature determination of $\pm 1$ K, which results in a 2% error. The total error is then the sum in quadrature of these three contributions, which should not exceed 15% (see Table I).

The linear fit line offset (Lorentzian width at $p=0$ torr) should correspond to the natural linewidth of 1.4 MHz. However, this is not the case in our measurements. Several effects contribute to the observed linear fit line offset value. First, any systematic error in temperature and pressure measurements strongly affects the linear fit line offset value. Second, Rb-Rb resonance broadening is not negligible since the small transition probability of the $5\,^2S_{1/2}$–$6\,^2P_{3/2}$ line imposes the need for raising Rb concentration above the room-temperature value (e.g., the reference cell and the HPO are heated). The result is Rb-Rb self-broadening of about 20 MHz [20]. The third effect includes finite laser linewidth and

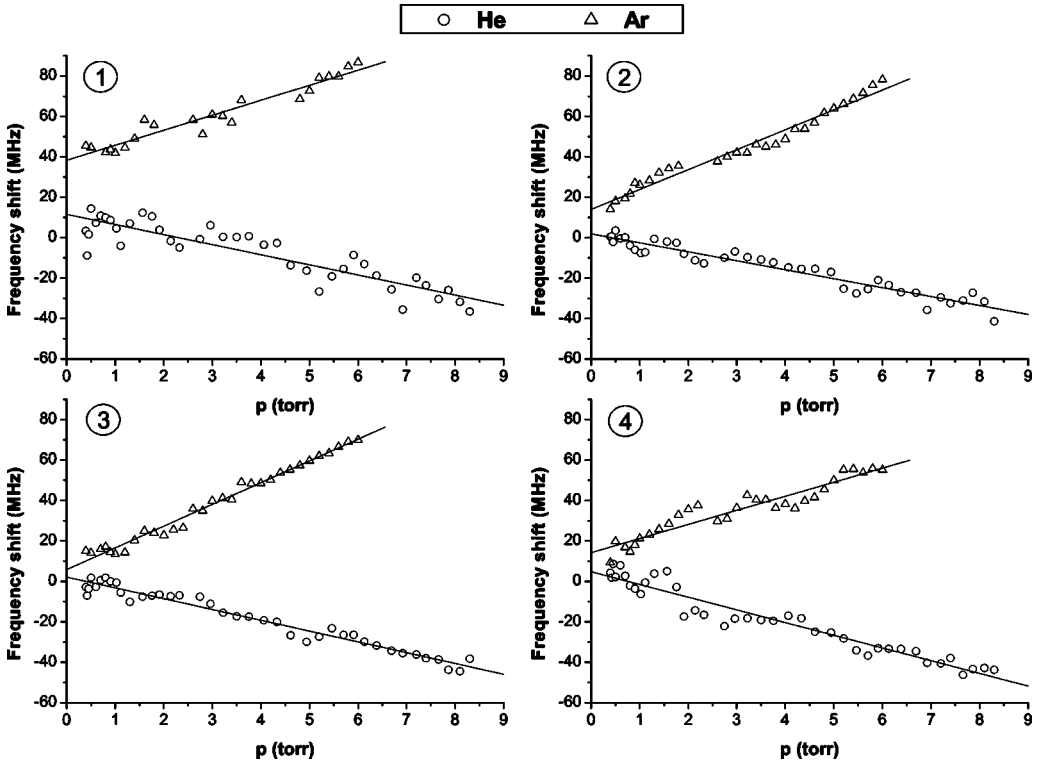


FIG. 4. The frequency shift results of the Rb $5\,^2S_{1/2}$–$6\,^2P_{3/2}$ line in He and Ar (hyperfine line notation the same as in Fig. 1).

the existence of stray magnetic fields, which could not be avoided in the experimental arrangement and results in an additional line broadening of about 10 MHz. The data presented in Fig. 3 were obtained by subtracting the observed Lorentzian linewidths in the reference cell from the corresponding ones measured in the HPO. In this way, the pressure broadening by noble gases was separated from all additional broadening mechanisms. As we are only interested in relative changes of the linewidths and shifts with the buffer-gas pressure, all additional line broadening mechanisms do

TABLE I. The results of pressure broadening and shift of the Rb $5\,^2S_{1/2}$–$6\,^2P_{3/2}$ line by He ($T$=368 K) and Ar (T=358 K).

| Buffer gas | Measured quantity | Hyperfine line | Value (MHz/torr) | Linear fit error (MHz/torr) | Total error (MHz/torr) |
|---|---|---|---|---|---|
| He | width | $^{87}$Rb $F=2\rightarrow1,2,3$ | 42.9 | 1.0 | 1.4 |
| | | $^{85}$Rb $F=3\rightarrow2,3,4$ | 48.8 | 0.7 | 1.3 |
| | | $^{85}$Rb $F=2\rightarrow1,2,3$ | 45.3 | 0.9 | 1.4 |
| | | $^{87}$Rb $F=1\rightarrow0,1,2$ | 53.6 | 1.6 | 2.0 |
| | shift | $^{87}$Rb $F=2\rightarrow1,2,3$ | −5.0 | 0.4 | 0.4 |
| | | $^{85}$Rb $F=3\rightarrow2,3,4$ | −4.4 | 0.2 | 0.2 |
| | | $^{85}$Rb $F=2\rightarrow1,2,3$ | −5.3 | 0.2 | 0.2 |
| | | $^{87}$Rb $F=1\rightarrow0,1,2$ | −6.3 | 0.3 | 0.3 |
| Ar | width | $^{87}$Rb $F=2\rightarrow1,2,3$ | 45.9 | 1.1 | 1.5 |
| | | $^{85}$Rb $F=3\rightarrow2,3,4$ | 30.5 | 1.1 | 1.3 |
| | | $^{85}$Rb $F=2\rightarrow1,2,3$ | 25.4 | 1.4 | 1.5 |
| | | $^{87}$Rb $F=1\rightarrow0,1,2$ | 30.9 | 4.6 | 4.6 |
| | shift | $^{87}$Rb $F=2\rightarrow1,2,3$ | 7.4 | 0.5 | 0.5 |
| | | $^{85}$Rb $F=3\rightarrow2,3,4$ | 9.9 | 0.3 | 0.4 |
| | | $^{85}$Rb $F=2\rightarrow1,2,3$ | 10.7 | 0.3 | 0.4 |
| | | $^{87}$Rb $F=1\rightarrow0,1,2$ | 7.0 | 0.5 | 0.5 |

not affect the calculated values of the pressure broadening and shift parameters (linear fit line slopes), but only the linear fit line offsets.

The frequency shifts show a linear dependence on the He and Ar buffer-gas pressure (Fig. 4). The slope of the linear fit to the measured data determines the frequency shift parameter value. The line offset (frequency shift at $p=0$ torr) should have zero value. The same arguments as in the case of the pressure broadening result in the nonzero line offset.

Finally, it should be pointed out that the accuracy of the numerical fit calculation is strongly affected by the shape of the absorption profiles themselves. This refers to the Doppler width (about 1000 MHz), which is large compared to the Lorentzian widths, therefore making any calculation of the Lorentzian widths less accurate. In addition to this, we used a large number of free parameters in the fitting procedure, which altogether may influence the total accuracy of our values shown in Table I.

In an attempt to avoid the effect of Doppler broadening, we performed Doppler-free saturation absorption measurements. Unfortunately, this method was not suitable for the pressure broadening and shift parameter determination, since the large crossover signals tend to mask the hyperfine lines of interest. Therefore, we are preparing new experiments with sufficiently dense rubidium vapor at very low temperatures. In addition, we shall use ultrathin cells with rubidium vapor in order to greatly reduce the influence of the Doppler broadening [21–23].

## V. CONCLUSION

We performed high-resolution measurements of the pressure broadening and shift of the rubidium $5\,^2S_{1/2}$–$6\,^2P_{3/2}$ (420.2 nm) spectral line by argon and helium buffer gases. To our knowledge, no similar experimental results with hyperfine line resolution exist for rubidium.

In general, the obtained pressure broadening and shift parameters have different values for different hyperfine components. At present, we are not aware of any interaction potential calculations at the level of hyperfine structure accuracy for the Rb-He and Rb-Ar systems. The existing calculations for Rb-Rb hyperfine potentials near the $5\,^2S_{1/2}$–$5\,^2P_{3/2}$ asymptote [24] indicate a very complex structure which may cause differences in line-shape parameters. It is reasonable to assume that similar, but somewhat simpler, situation should apply to Rb-He and Rb-Ar cases, causing differences in the broadening and shift parameters of relevant hyperfine lines.

The effect of different noble gas used as the perturber may be perceived through the larger value of the pressure broadening parameter for He. In addition, the $5\,^2S_{1/2}$–$6\,^2P_{3/2}$ line shifts toward the red in He, corresponding to the attractive "effective" Rb-He potential, whereas in Ar the line shifts toward the blue, pointing to the fact that Rb-Ar "effective" potential is repulsive [25].

## ACKNOWLEDGMENTS

We acknowledge the support from the Ministry of Science and Technology of the Republic of Croatia, the European Community Research Training Network (FW-5), and the Alexander von Humboldt Foundation.

[1] H. Margenau and W. W. Watson, Rev. Mod. Phys. **8**, 22 (1936).
[2] S. Y. Ch'en and M. Takeo, Rev. Mod. Phys. **29**, 20 (1957).
[3] N. Allard and J. Kielkopf, Rev. Mod. Phys. **54**, 1103 (1982).
[4] E. L. Lewis, Phys. Rep. **58**, 1 (1980).
[5] W. Happer, Rev. Mod. Phys. **44**, 169 (1972).
[6] A. Burrows and M. Volobuyev, Astrophys. J. **583**, 985 (2003).
[7] A. Andalkar and R. B. Warrington, Phys. Rev. A **65**, 032708 (2002).
[8] Ch. Ottinger, R. Scheps, G. W. York, and A. Gallagher, Phys. Rev. A **11**, 1815 (1975).
[9] B. L. Bean and R. H. Lambert, Phys. Rev. A **12**, 1498 (1975).
[10] M. V. Romalis, E. Miron, and G. D. Cates, Phys. Rev. A **56**, 4569 (1997).
[11] T. Z. Ny and S. Y. Ch'en, Phys. Rev. **52**, 1158 (1937).
[12] D. H. Sarkisyan, A. S. Sarkisyan, and A. K. Yalanusyan, Appl. Phys. B: Lasers Opt. **66**, 241 (1998).
[13] D. Aumiler, T. Ban, R. Beuc, and G. Pichler, Appl. Phys. B: Lasers Opt. **76**, 859 (2003).
[14] K. B. MacAdam, A. Steinbach, and C. Wieman, Am. J. Phys. **60**, 1098 (1992).
[15] R. J. Wells, J. Quant. Spectrosc. Radiat. Transf. **62**, 29 (1999).
[16] A. Corney, *Atomic and Laser Spectroscopy* (Clarendon, Oxford, 1977), p. 718.
[17] Y. Dancheva, G. Alzetta, S. Cartaleva, M. Taslakov, and Ch. Andreeva, Opt. Commun. **178**, 103 (2000).
[18] A. Hemmerich, D. H. Mclntyre, C. Zimmermann, and T. W. Hänsch, Opt. Lett. **15**, 372 (1990).
[19] P. Grundevik, M. Gustavsson, A. Rosen, and S. Svanberg, Z. Phys. A **283**, 127 (1977).
[20] W. Demtröder, *Laser Spectroscopy* (Springer-Verlag, Berlin, 2003), p. 77.
[21] D. Sarkisyan, D. Bloch, A. Papoyan, and M. Ducloy, Opt. Commun. **200**, 201 (2001).
[22] D. Sarkisyan, A. Papoyan, T. Varzhapetyan, J. Alnis, K. Blush, and M. Auzinsh, J. Opt. A, Pure Appl. Opt. **6**, S142 (2004).
[23] D. Sarkisyan, T. Becker, A. Papoyan, P. Thoumany, and H. Walther, Appl. Phys. B: Lasers Opt. **76**, 625 (2003).
[24] M. Kemmann, I. Mistrik, S. Nussmann, and H. Helm, Phys. Rev. A **69**, 022715 (2004).
[25] K. Niemax and G. Pichler, J. Phys. B **7**, 2355 (1974).